

Island Shape Controls Magic-Size Effect for Heteroepitaxial Diffusion

Henry H. Wu, A. W. Signor, and Dallas R. Trinkle*

Department of Materials Science and Engineering,

University of Illinois, Urbana-Champaign

(Dated: April 2, 2024)

Abstract

Lattice mismatch of Cu on Ag(111) produces fast diffusion for special “magic sizes” of islands. A size- and shape-dependent reptation mechanism is responsible for low diffusion barriers. Initiating the reptation mechanism requires a suitable island shape, a property not considered in previous studies of 1D island chains and 2D closed-shell islands. Shape determines the dominant diffusion mechanism and leads to multiple clearly identifiable magic-size trends for diffusion depending on the number of atoms whose bonds are shortened during diffusion.

PACS numbers: 68.35.Fx, 68.35.bd, 68.35.Gy, 71.15.Pd

Control of thin-film morphology relies on understanding multiple ongoing processes during deposition and growth. In particular, diffusion of small atom clusters on surfaces play a critical role in thin film growth, especially in early stages. The diffusion kinetics of small islands in heteroepitaxial systems is less well understood than that of homoepitaxial diffusion, for which much experimental[1, 2, 3, 4] and theoretical[5, 6, 7, 8] work has been done. Strain is known to govern the mesoscale morphology in self-assembling systems[9]. While predictions about the role of size and misfit for small islands go back over a decade[10], only recent experiments have captured and quantified the rapid diffusion at “magic sizes” in the heteroepitaxial Cu/Ag(111) system[11]. However, the experimental observations of rapid diffusion from several distinct sizes of islands does not easily comport with the simple model of Hamilton for magic sizes. A missing element in explaining the atomistic diffusion mechanism is the role of island shape in controlling diffusion. Understanding the trends of diffusion barriers for small islands with island size and shape for the common cubic (111) surface provides insight for experimental measurements and thin-film growth, and provides the fundamental understanding to control morphology.

Hamilton predicted a magic-size effect for heteroepitaxial islands with a one-dimensional Frenkel-Kontorova model[12] and a corresponding two-dimensional equivalent[10]. The 1D model describes a chain of atoms harmonically coupled to their neighbors and interacting with a rigid periodic substrate potential. The lattice misfit is the percentage difference between the equilibrium spring length and the substrate periodicity, and the island misfit strain grows linearly with the number of atoms in the island chain. The diffusion barrier has non-monotonic behavior with size, showing a minimum at the “magic size” equal to inverse of the lattice misfit. At this size, the island ground-state configuration contains one dislocation, where island atoms sit at a peak of the substrate potential instead of a valley. Islands below the magic size are dislocation-free with a large energy barrier to nucleate and propagate a dislocation for island diffusion, while larger islands contain a dislocation and require an increasing energy barrier to move this dislocation for island diffusion. Using the embedded atom method (EAM[13]) for Ag/Ru(0001), Hamilton considered a 2D equivalent with closed-shell islands, and the magic size corresponds with the ground-state configuration containing one dislocation[10]. The ground state has atoms displaced from FCC to HCP sites on the hexagonal Ru(0001) surface. The dislocation line marks the separation between FCC and HCP sections of the island. Diffusion for these islands proceeds as all atoms in the island collectively glide to continuously propagate the dislocation.

Reptation—first proposed for small island diffusion in homoepitaxial systems—relies on dis-

location movement[14]. Unlike Hamilton’s collective glide mechanism, reptation proceeds as the motion of an island section from FCC to HCP sites on the (111) surface, forming a dislocation where the island atomic bonds are stretched. Diffusion is completed after the remaining island section subsequently follows in the same direction to complete the transition. Therefore the reptation dislocation propagates through sequential motion of island sections while the collective glide dislocation propagates by the continuous motion of the entire island.

We find that the reptation diffusion mechanism exhibits a magic-size effect in Cu/Ag(111) controlled by island shape that explains experimental observations of anomalous diffusion. Using an optimized EAM potential with molecular dynamics and the dimer method, we calculate island diffusion barriers up to 14-atom islands. The diffusion barriers of different island sizes and shapes is a non-monotonic function of the island misfit strain, and separates into simple groups depending on the geometry of the island. The shape effect is explained by the continuity of bonds during diffusion. We find that the reptation mechanism is competitive over the glide mechanism for all islands except those with closed-shell shapes. After considering the modulating effect of island geometry and the competition between the diffusion mechanisms, we find multiple magic sizes each diffusing with a single dislocation. By considering island shape, we predict a series of rapidly diffusing islands, each as their own magic size.

Our study of island diffusion relies on an EAM potential optimized for the prediction of island geometries, energetics, and kinetics for Cu/Ag(111)[15]. The potential was optimized using monomer and dimer DFT energies and geometries. The optimized EAM predicts the DFT monomer diffusion barrier and the DFT energy difference between all-FCC trimers and all-HCP trimers. However the potential (and DFT) overestimates the monomer and dimer diffusion barriers at 93 and 88meV compared to experimental[16] values of 65 ± 9 and 73meV, respectively. This is a carryover from DFT which has been shown to overestimate surface adsorption energies[17]. Due to this discrepancy, we present our calculated island diffusion barriers relative to the monomer diffusion barrier $E_{\text{diff}}^{\text{monomer}}$ of 93meV.

We anneal to determine island ground-state structures, and use molecular dynamics[18], dimer-search[19], and nudged elastic band[20] method to find island diffusion transitions and determine diffusion barriers. Multiple annealing runs for each island size reveal compact islands with all FCC-site ground-states for small sizes while mixed FCC/HCP ground-states exist only for the 13- and 14-atom islands, the largest in our study. We run direct molecular dynamics at high temperature (600K) over several nanoseconds to explore possible transitions. We also use the dimer

method which randomly searches through phase-space for possible transitions from a starting state. Nudged elastic band finds the minimum energy pathway between the starting and ending states of discovered transitions and extracts the diffusion barrier.

Different island shapes are possible for each island size in 2D, while two different sites on the (111) surface allows different energies for the same shape. The islands form compact ground-state configurations that maximize atomic coordination and minimize island strain. The triangular (111) surface lattice contains two hexagonal sublattices—FCC and HCP—each with lattice spacing equal to that of the Ag nearest neighbor distance $nn_{\text{Ag}} = 2.89\text{\AA}$. A FCC-site is surrounded by three HCP-sites in the $\langle 11\bar{2} \rangle$ directions, while the next nearest FCC-sites are in the close-packed $\langle \bar{1}10 \rangle$ directions. Cu islands, with bulk nearest neighbor distance $nn_{\text{Cu}} = 2.56\text{\AA}$, experience large misfit strains if all the island atoms sat exclusively on one sublattice. However, since FCC-sites are closer to neighboring HCP-sites, the total island strain can be reduced if some atoms in the island sit in a mixed FCC-HCP (FH) bond with a lattice site distance of only $\frac{1}{\sqrt{3}}Ag_{mn} = 1.67\text{\AA}$ rather than the longer FCC-FCC (FF) or HCP-HCP (HH) bonds. For a system with an opposite lattice mismatch we would expect the next nearest neighbor FH-bonds with a lattice site distance of $\frac{2}{\sqrt{3}}Ag_{mn} = 3.34\text{\AA}$; this is also the case in the Pt/Pt(111) system[14].

We measure the substrate strain in each island in terms of the island misfits in Fig. 1. We relax ground-state configurations of different islands and calculate the surface strain as a function of distance away from the island’s center-of-mass. The atomic strain tensor for each surface Ag atom is an average over the change in all nearest-neighbor vectors[21]. In Fig. 1a the tensile normal strain—sum of ϵ_{xx} and ϵ_{yy} —drops off as the inverse squared radial distance from the island’s center-of-mass and scales with island size; we define the scaling coefficient as the island misfit, which has units of area. This island misfit with the substrate varies with the size and shape, and in Fig. 1b, we find a linear correlation with the island size. We use the island misfit as a measure of the strain in the island because it contains information about both the island size and shape. Other island growth studies used the a related measure of the substrate stress instead of strain[22], which is linearly related. This measure of substrate strain accounts for the effect of island shape, and helps relate the 2D system back to the simpler 1D model.

Islands diffuse by the passage of a dislocation, with two different forms in 2D: collective glide (Fig. 2b), or reptation (Fig. 2a). Collective glide is the mechanism described by Hamilton, where the dislocation propagates with the continuous motion of the entire island moving from FCC to HCP sites, or vice versa. Closed-shell configurations (3-, 7-, and 12-atom islands) favor the col-

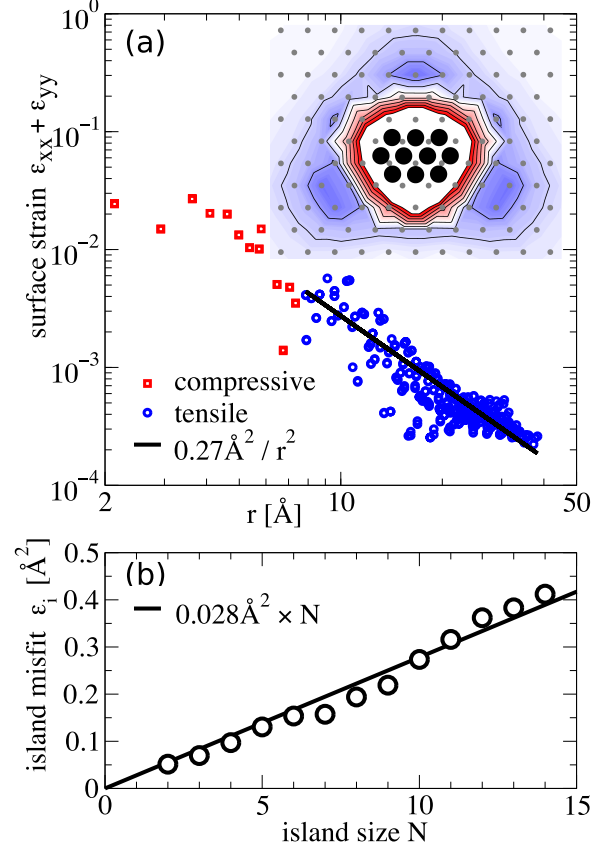


FIG. 1: Cu islands and strain in the Ag(111) surface. (a) Magnitude of the atomic strain plotted against the radial distance from the 10-atom island center-of-mass. The tensile strain $\epsilon_{xx} + \epsilon_{yy}$ is the inverse squared radial distance times the island misfit ϵ_i . The inset shows the hydrostatic strain induced by the ground-state 10-atom Cu island in the Ag surface. Compressive strain is in red (strains exceed -1.0% under the island and are not shown), and the compensating tensile strain is in blue. (b) The island misfit ϵ_i of ground-state island configurations grows linearly with island size N as $0.028 \text{ Å}^2 \times N$, while modulations show the influence of island shape.

lective glide mechanism, which maintains neighboring bonds during diffusion. Reptation involves sequential motion of island sections to HCP sites, via a metastable dislocated structure. The FCC portion of the metastable state is separated from the HCP portion by a dislocation with a $\langle \bar{1}10 \rangle$ -type line direction. We identify this dislocation line direction to be characteristic of the reptation mechanism. Island shape is the critical criteria to determine whether a 2D island prefers the collective glide mechanism or the reptation mechanism.

Fig. 2 shows the geometric requirement to undergo the reptation mechanism at a low energy barrier: no atom should be left without a bond across the dislocation line. The reptation mechanism

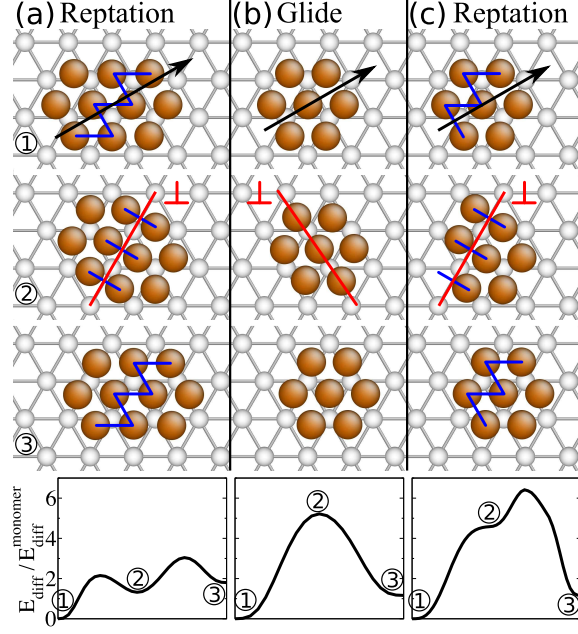


FIG. 2: Geometric requirements for low barrier island reptation diffusion. A Δ of Ag surround the FCC surface site and ∇ for the HCP surface site. (a) An **allowed** reptation transition involves transforming homogeneous bonds (1) into heterogeneous bonds (2) *without* leaving an unbonded Cu atom. This is a necessary condition for the reptation dislocation mediated island diffusion. (b) The collective glide dislocation mediated diffusion mechanism observed for the 7-atom island. Atoms shuffling in the direction of diffusion propagates the passing dislocation (2). (c) A **disallowed** reptation transition for the 7-atom island leaves one Cu atom without a bond across the dislocation line (2) and is high in energy. The energy barrier pathway for all three transitions is shown below normalized with respect to the EAM monomer diffusion barrier of 93meV.

slips part of the island onto HCP sites where the number of $\langle \bar{1}10 \rangle$ island rows sheared by the dislocation line form the same number of heterogeneous FH-bonds (Fig. 2a.2). The energy cost to form FH-bonds and move atoms to HCP sites is compensated by the reduction of island strain from the smaller island area of the dislocated state. For the 10-atom island shown, the island misfit is reduced from 0.27\AA^2 (Fig. 2a.1) to 0.22\AA^2 (Fig. 2a.2). An island with unequal number of atoms across the dislocation line—two facing three in the 7-atom island—has to overcome the additional barrier to break a bond during island shear (Fig. 2c.2). The dimer dissociation energy for Cu on Ag(111) is $370\text{meV} \approx 4E_{\text{diff}}^{\text{monomer}}$, which increases the reptation mechanism energy barrier for closed-shell islands above the collective glide mechanism barrier. Ultimately, the absence of bond-breaking during slip is the deciding factor in allowing a low energy reptation mechanism.

Fig. 3 groups barriers for islands with equal numbers of sheared $\langle \bar{1}10 \rangle$ rows, demonstrating the shape-modulated magic-size effect. For reptation-allowed islands, this groups islands with the same number of FH-bonds in the dislocated state, and for reptation-disallowed islands this is the number of $\langle \bar{1}10 \rangle$ rows in the diffusion direction. The 2- and 3-row groups appear very similar to the characteristic magic-size effect plot for 1D island chains diffusion[10]. The 7- and 8-atom island configurations in the 2-row group are not ground-states and are constructed to test the continuation of the 2-row magic-size effect. The shape of these two islands induce larger strains than in their ground-states and promotes the dramatic reduction in diffusion barrier. The shape effect from sheared $\langle \bar{1}10 \rangle$ rows gives different magic-size regions even though only one dislocation is present in all cases.

The transition pathways for 2D islands of different row-groups in Fig. 3 also follow the trends seen for the 1D island chains. In the 2-row group, the dislocated state is not metastable for the 4-atom island and becomes more and more stable with increasing island size. The dislocated state of the 7-atom 2-row is almost equal in energy with the undislocated state, while the dislocated state of the 8-atom 2-row is the ground state and possesses a higher diffusion barrier. In the 3-row group, the dislocated state is not metastable for the both the 8- and 9-atom islands and becomes metastable at 10-atoms. Continuing the 3-row group, the dislocated state of the 11-atom island is still metastable, but the diffusion barrier is higher due to asymmetric island structure. Finally, the dislocated state for the 13-atom island is the ground-state and the diffusion barrier becomes even higher. The minima for ground-state diffusion barriers—6- and 10-atom islands—corresponds well with experimental observations, as well as the immobility of 7-atom islands[11].

Island shape controls the 2D magic-size effect for Cu/Ag(111) where a combination of island geometry and misfit produces multiple magic sizes even for single dislocation-mediated diffusion. We find that the reptation diffusion mechanism allows for greatly reduced diffusion barriers for heteroepitaxial systems compared with the collective glide mechanism. The criteria for the reptation mechanism requires the island shape to be such that no atom is left unbonded across the dislocation line. This mechanism predicts multiple magic sizes even for small (< 20) island sizes, which quantitatively agrees with experimental observations of Cu/Ag(111). We expect similar effects in other heteroepitaxial systems with large lattice misfits, and for the magic size islands to affect the growth morphologies for low coverages.

The authors thank John Weaver for helpful discussions. This research is supported by NSF/DMR grant 0703995, and 3M's Untenured Faculty Research Award.

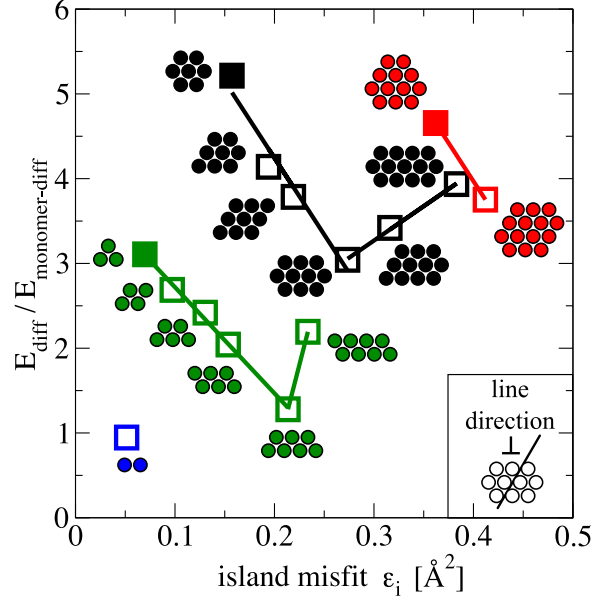


FIG. 3: The island diffusion barriers versus island misfit ϵ_i for different islands showing a shape-modulated magic-size effect. The diffusion barrier is normalized with respect to the EAM monomer diffusion barrier of 93meV. The open symbols represent islands that allow reptation according to their shape, while the filled symbols are islands that do not (the configurations shown are oriented with respect to the dislocation line direction in the inset). Islands with the same number of sheared $\langle \bar{1}10 \rangle$ rows along the dislocation line follow a “magic size” trend in barriers as a dislocation aids in diffusion—with blue for 1-, green for 2-, black for 3-, and red for 4-rows. The distinct groupings of magic-size regions highlight the key role of shape in the diffusion of small islands with a large lattice misfit. The 7- and 8-atom 2-row configurations in green are not energetically favorable, but show the continuation of the 2-row magic-size effect. Note: The glyphs shown for the 6-, 9- and 11-atom islands are not the ground-state configurations for that size, but instead represent the shape before a diffusion transition.

* Electronic address: dtrinkle@illinois.edu

- [1] J.-M. Wen, S.-L. Chang, J. W. Burnett, J. W. Evans, and P. A. Thiel, Phys. Rev. Lett. **73**, 2591 (1994).
- [2] G. L. Kellogg and A. F. Voter, Phys. Rev. Lett. **67**, 622 (1991).
- [3] M. C. Bartelt, C. R. Stoldt, C. J. Jenks, P. A. Thiel, and J. W. Evans, Phys. Rev. B **59**, 3125 (1999).
- [4] G. Antczak and G. Ehrlich, Surface Science Reports **62**, 39 (2007).
- [5] N. I. Papanicolaou, G. A. Evangelakis, and G. C. Kallinteris, Computational Materials Science **10**,

105 (1998).

- [6] F. Montalenti and R. Ferrando, Phys. Rev. B **59**, 5881 (1999).
- [7] A. Bogicevic, Phys. Rev. Lett. **82**, 5301 (1999).
- [8] H. T. Lorensen, J. K. Nørskov, and K. W. Jacobsen, Phys. Rev. B **60**, R5149 (1999).
- [9] N. V. Medhekar, V. B. Shenoy, J. B. Hannon, and R. M. Tromp, Phys. Rev. Lett. **99**, 156102 (2007).
- [10] J. C. Hamilton, Phys. Rev. Lett. **77**, 885 (1996).
- [11] A. W. Signor, H. H. Wu, and D. R. Trinkle (2009), URL <http://arxiv.org/abs/0908.3004>.
- [12] S. Aubry and P. Y. L. Daeron, Physica D **8**, 381 (1983).
- [13] S. M. Foiles, M. I. Baskes, and M. S. Daw, Phys. Rev. B **33**, 7983 (1986).
- [14] V. Chirita, E. Munger, J. Greene, and J.-E. Sundgren, Surface Science Letters **436**, L641 (1999).
- [15] H. H. Wu and D. R. Trinkle (2009), URL <http://arxiv.org/abs/0901.0861>.
- [16] K. Morgenstern, K.-F. Braun, and K.-H. Rieder, Phys. Rev. Lett. **93**, 056102 (2004).
- [17] C. Stampfl, Catalysis Today **105**, 17 (2005).
- [18] S. J. Plimpton, J. Comp. Phys. **117**, 1 (1995), URL <http://lammps.sandia.gov/index.html>.
- [19] G. Henkelman and H. Jónsson, J. Chem. Phys. **111**, 7010 (1999).
- [20] G. Mills and H. Jónsson, Phys. Rev. Lett. **72**, 1124 (1994).
- [21] P. M. Gullett, M. F. Horstemeyer, M. I. Baskes, and H. Fang, Modelling Simul. Mater. Sci. Eng. **16** (2008).
- [22] C.-W. Pao and D. J. Srolovitz, Journal of the Mechanics and Physics of Solids **54**, 2527 (2006).